Research Article

TRR
JOURNAL OF THE TRANSPORTATION RESEARCH BOARD

Transportation Research Record
1–9

DOI: 10.1177/0361198120945597
journals.sagepub.com/home/trr
SAGE

Driver Reactions to Uphill Grades: Inference from a Stochastic Car-Following Model

Tu Xu[1] and Jorge Laval[1]

Abstract

This paper analyzes the impact of uphill grades on the acceleration drivers choose to impose on their vehicles. Statistical inference is made based on the maximum likelihood estimation of a two-regime stochastic car-following model using Next Generation SIMulation (NGSIM) data. Previous models assume that the loss in acceleration on uphill grades is given by the effects of gravity. We find evidence that this is not the case for car drivers, who tend to overcome half of the gravitational effects by using more engine power. Truck drivers only compensate for 5% of the loss, possibly because of limited engine power. This indicates not only that current models are severely overestimating the operational impacts that uphill grades have on regular vehicles, but also underestimating their environmental impacts. We also find that car-following model parameters are significantly different among shoulder, median and middle lanes but more data is needed to understand clearly why this happens.

Modeling truck performance with roadway grade has a long history. In the 1970s researchers collected speed and weight data for trucks operating on highway grades (*1*). Based on the data, they found that trucks experienced great acceleration loss on uphill segments and the magnitude of acceleration loss depended on the approach speed. Later, the previous research was extended by Gillespie (*2*), who developed a methodology to predict truck acceleration loss on grades for different classes of trucks. These studies for designing climbing lanes only consider the tangent vertical profiles, so Yu (*3*) focused on the impact of vertical curvature on truck performance.

The impact of the roadway grade on passenger cars has long been neglected. In the AASHTO report (*4*), the authors point out that passenger cars can generally negotiate a grade of 5% or less without significant acceleration loss. Modeling work to incorporate roadway grade with vehicle acceleration can be found in Laval (*5*), who argued that roadway grade is a key ingredient to produce traffic instabilities as observed empirically. In that study, the crawl speed for both passenger cars and trucks was calculated based on the free motion model from McLean (*6*). Later, Laval et al. successfully replicated periodic oscillations at uphill segments with a car-following model that included the effects of gravity (*7*). They assumed that on an upgrade segment the acceleration because of gravity in the direction of movement, gG, is subtracted from the acceleration a driver would have imposed on a vehicle on a flat segment. However, this assumption implies that drivers do not press the gas pedal harder on uphill segments, which may not be the actual case, as reported in Ros et al. (*8*). That study presented a novel car-following model along with a lane-changing model and found that the influence of roadway grade on vehicle longitudinal motion is more realistic than that predicted by existing models (*8*). However, the study did not investigate the difference among vehicle classes and more data are needed for calibration and validation.

The purpose of this paper is to test the effect of roadway grade on vehicles and find the difference between regular vehicles and trucks. To this end, this paper is organized as follows. First the model is introduced, then the US 101 dataset is used to estimate model parameters and statistical tests are performed. At the end of the paper, a discussion and conclusions are provided.

Background

The model used in this paper is the two-regime stochastic car-following model of Xu and Laval (*9*, *10*). It corresponds to an extension of Newell's simplified

[1]Georgia Tech, Atlanta, GA

Corresponding Author:
Jorge Laval, jorge.laval@ce.gatech.edu

car-following theory (*11*), where vehicle location is given by the minimum of a free-flow term expressing the location (Y) that the vehicle can achieve when unobstructed by traffic, and a congestion term giving the most downstream location (Z) that the vehicle can safely achieve without colliding with its leader. It can be formulated as:

$$x_j(t) = \min\{\underbrace{x_j(t-\tau) + \xi_j(\tau)}_{\text{free-flow (Y)}}, \underbrace{x_{j-1}(t-\tau) - \delta}_{\text{congestion (Z)}}\}, \quad (1)$$

where $x_j(t)$ is the position of j -th vehicle at time t, τ is the wave trip time between two consecutive vehicle trajectories in congestion, δ is the jam spacing and $\xi_j(\tau)$ is a stochastic process describing the desired displacement of vehicle j during $t-\tau$ and t. Notice that τ is typically taken as the time step of the car-following model.

The free-flow term Y in the proposed acceleration model (*9*, *10*) is as follows:

$$\begin{cases} d\xi(t) = v(t)dt, \qquad \xi(0) = 0, & (2a) \\ dv(t) = (v_c - v(t))\beta dt + (mv_c - v(t))\sigma dW(t), \\ v(0) = v_0 & (2b) \end{cases}$$

and has analytical solution where $v(t)$ is the current vehicle speed, v_c is the desired speed, β is the inverse relaxation time, m is a dimensionless parameter that regulates acceleration error, $W(t)$ is a standard Brownian Motion and σ is its diffusion coefficient. A normalized diffusion coefficient $\tilde{\sigma}$ is introduced by $\tilde{\sigma}^2 = \sigma^2/\beta$.

In the congestion part Z of the model, wave trip time τ and δ are assumed to follow the bivariate normal (BVN) distribution (*12*), that is:

$$(\tau, \delta) \sim \mathrm{BVN}(\mu_\tau, \mu_\delta, \sigma_\tau, \sigma_\delta, \rho).$$

Since random processes Y and Z are normally distributed: $Y \sim N(\mu_Y, \sigma_Y)$, $Z \sim N(\mu_Z, \sigma_Z)$, one can show that the probability density function of $x_j(t)$, $f(x;\Theta)$, given the data up to time t and the set of model parameters $\Theta = (u, \mu_\tau, \mu_\delta, \beta, m, \tilde{\sigma}, \rho, \sigma_\tau, \sigma_\delta)$, is given by

$$f(x;\Theta) = \frac{1}{2\sqrt{2\pi}} \left(\frac{1}{\sigma_Z} e^{-\frac{(\mu_Z - x)^2}{2\sigma_Z^2}} \operatorname{erfc}\left(\frac{x-\mu_Y}{\sqrt{2}\sigma_Y}\right) + \frac{1}{\sigma_Y} e^{-\frac{(\mu_Y - x)^2}{2\sigma_Y^2}} \operatorname{erfc}\left(\frac{x-\mu_Z}{\sqrt{2}\sigma_Z}\right) \right) \quad (3)$$

where $\operatorname{erfc}(x) = \frac{2}{\sqrt{\pi}}\int_x^\infty e^{-t^2}\,dt$ is the complementary error function. The mean and standard deviations of the free-flow and congestion terms are given by:

$$\begin{cases} \mu_Y = x_j(t_i - \tau') + \mathrm{E}[\xi(\tau')], & (4a) \\ \sigma_Y = \mathrm{SD}[\xi(\tau')], & (4b) \\ \mu_Z = x_{j-1}(t_i - \mu_\tau) - \mu_\delta, & (4c) \\ \sigma_Z = \sqrt{v_{j-1}^2(t_i)\sigma_\tau^2 + \sigma_\delta^2 + 2\rho v_{j-1}^2(t_i)\sigma_\tau^2\sigma_\delta^2}. & (4d) \end{cases}$$

which is all we need to evaluate Equation 3 and use maximum likelihood estimation (MLE) to estimate the parameters. For details of the model and parameter estimation, the reader is referred to Xu and Laval (*9*, *10*).

Modeling Vehicle Acceleration with Roadway Grade

In this model, the mean of vehicle acceleration is:

$$a(v) = (v_c - v(t))\,\beta, \quad (5)$$

On a flat road, v_c equals the free-flow speed u. To take the upgrade of the roadway into account, we replace Equation 5 by

$$a(v) = (u - v(t))\,\beta - \alpha g \max\{0, G\}, \quad (6)$$

where u is the free-flow speed, that is, the desired speed on a flat road segment, $g = 9.81\,\mathrm{m/s}^2$ is the acceleration of gravity, G is the roadway grade expressed as a decimal and α is a dimensionless parameter. Notice that in existing free-motion acceleration models (*7*), $\alpha = 1$, which is consistent with the assumption that the acceleration because of gravity in the direction of movement, $g\max\{0, G\}$, is subtracted, in its entirety, from the acceleration the driver would impose on the vehicle on a flat segment, $(v_c - v(t))\,\beta$. Here, the parameter α is added to relax this strong assumption in the literature: $\alpha < 1$ indicates drivers compensate for the upgrade, that is, that they press the gas pedal harder than they would on a flat segment, while $\alpha > 1$ implies a softer than usual pressure. Values of $\alpha < 0$ are unlikely as it would indicate that acceleration increases with the upgrade.

Notice that the desired speed becomes a function of the upgrade, and can be expressed as:

$$v_c = u - \alpha g \max\{0, G\}/\beta. \quad (7)$$

Data Set

Trajectory Data

The Next Generation SIMulation (NGSIM) datasets contain detailed and accurate field data for traffic research and development. In this paper, we use the U.S. Highway 101 (US 101) dataset, which contains detailed vehicle trajectory data on southbound US 101, also known as the Hollywood Freeway, in Los Angeles, CA, collected on June 15, 2005. The length of the study segment is approximately 640 m (2,100 ft). There are five mainline lanes throughout the section and one auxiliary lane through a portion of the corridor between the on-ramp at Ventura Boulevard and the off-ramp at Cahuenga Boulevard (see Figure 1). This dataset provides the precise location of each vehicle area every one-tenth of a second during

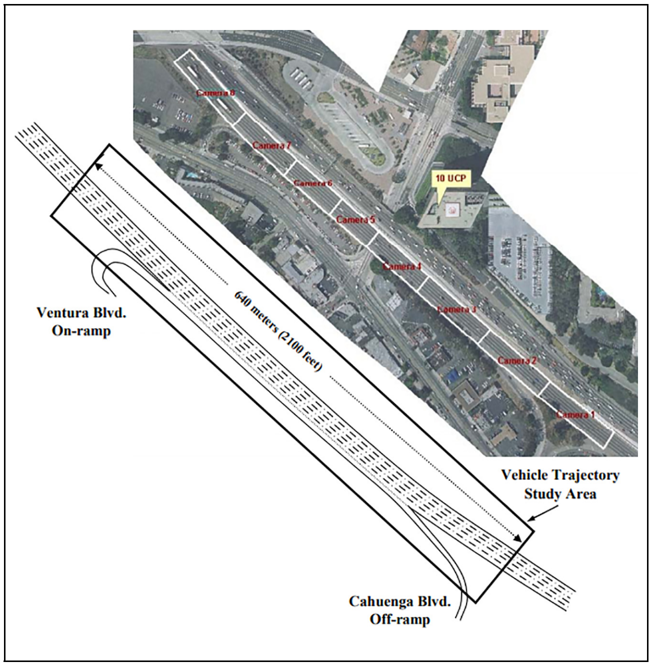

Figure 1. The site for US 101 data collection (*13*).

45 min in the morning peak hour. This period includes uncongested and congested traffic states and the transition between these two states (*13*).

Time–space diagrams of the vehicle trajectories are given the Figure 2. In Figure 2, the distance of each vehicle is drawn against time; the slope of the trajectory indicates the vehicle's speed. The green color represents a free-flow state and the red color represents a congested state. Periodic traffic congestion can be observed from the visualization of the dataset.

Grade Data

Modeling vehicle acceleration with roadway grade requires high-accuracy grade data. In this study, Google Earth was used to obtain the elevation profile along the study corridor, and the grade data was derived using a second-order interpolation, see Figure 2. The grade data in this study was verified with the USGS National Elevation Dataset (*14*) and it was concluded that the data is valid for this study. One can see that the segment has an average upgrade of around 2%, with larger grades near the beginning of the segment. Also note in this figure that the oscillations are not caused by the grade, but by a crew of workers located near the 400 m mark, as reported in (*15*).

Sample Size

The data used is from five mainline lanes during the period 7:50–8:05 a.m. Lane 1 is the leftmost lane and Lane 5 is the rightmost lane. Vehicles that performed lane changing during the period were removed. The remaining vehicles are used in the parameter estimation.

For vehicle i, if it entered the study corridor at t_{enter} and left the study corridor at t_{leave}, 50 uniform random variables can be generated, $t_1, t_2, \ldots t_{50}$, between t_{enter} and t_{leave} as the sample time stamp, such that there will be 50 sample points for one vehicle. Fifty sample points are selected from each vehicle to obtain as many sample points as possible while avoiding too much duplication. The 50 sample points are later randomly divided into five groups and each data point has different vehicle speed, roadway grade and other parameter values. This sampling method help increase sample size while preventing serial correlation from one vehicle. Table 1 summarizes the sample size for the parameter estimation for each lane, each vehicle class.

Data for each vehicle are randomly divided into five groups, each with a size of 10. Four groups (80% of the data) are used as training data and the remainder group (20% of the data) as validation data. For the four groups of training data, maximum likelihood is used to estimate parameter values, then the results from the four training groups are applied separately to the validation data. The estimation result that gives the biggest log-likelihood value on the validation data is selected as the final estimation result.

Data Set

This stochastic car-following model has the parameters summarized in Table 2:

MLE is used for the estimation of parameters in the proposed model. In a nutshell, MLE consists in finding the value of Θ that maximizes the log-likelihood $\ell(x; \Theta) = \sum_{i,j} \ln[f(x_j(t_i); \Theta)]$.

This gives the MLE estimator of Θ, and is denoted $\widehat{\Theta}$. MLE is appealing because, for large samples, one can perform statistical inference analysis to answer important questions in car-following behavior. For large samples the distribution of MLE estimators tends to the multivariate normal distribution, that is, $\widehat{\Theta} \overset{\text{dist}}{\rightarrow} N(\Theta, \Theta)$, where the covariance matrix Θ can be approximated using the Cramer-Rao lower bound: $\Theta \approx J(\widehat{\Theta})^{-1}$ where $J(\Theta) = -\frac{\partial^2 \ell(\Theta)}{\partial \Theta^2}$ is the observed Fisher's information for the sample. This important result allows us to use the statistical inference toolbox, in particular, confidence intervals and hypothesis testing.

Hypothesis Testing

A likelihood-ratio test can be used to compare the goodness-of-fit of different model specifications. For example, if we have two models with number of

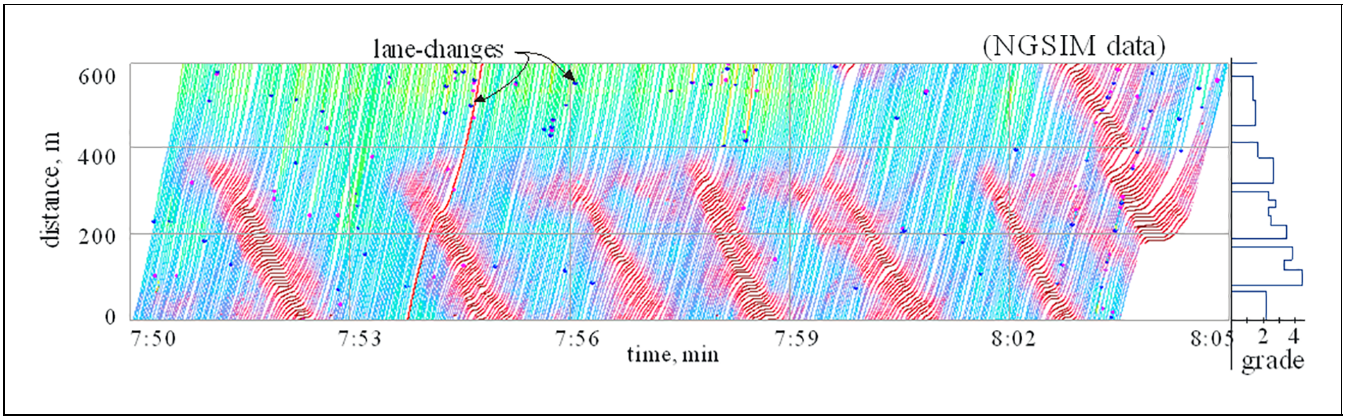

Figure 2. A visualization of the US 101 dataset (7).
Note: NGSIM = Next Generation SIMulation.

Table 1. Number of Sample Points for Parameter Estimation (50 Sample Points per Vehicle)

Lane	Motorcycles	Cars	Trucks	Total
1	300	13,450	50	13,800
2	150	10,750	0	10,900
3	0	9,150	200	9,350
4	100	6,650	100	6,850
5	50	5,800	100	5,950
Total	600	45,800	450	46,850

Table 2. Parameters in the Model

Parameter	Unit	Meaning
u	km/h	free-flow speed
β	hour $^{-1}$	inverse relaxation time.
m	na	regulates acceleration error
$\tilde{\sigma}$	na	normalized diffusion coefficient
μ_δ	meter	mean jam spacing
μ_τ	second	mean wave trip time
ρ	na	correlation between δ, τ
σ_δ	meter	standard deviation of jam density
σ_τ	second	standard deviation of wave trip time
α	na	upgrade parameter

Note: na = not applicable.

parameters n_1 and n_2 $(n_1 > n_2)$, respectively, the likelihood-ratio test statistic is $\Lambda(\mathbf{x}) = 2\left[\ell(\mathbf{x}; \widehat{\Theta_1}) - \ell(\mathbf{x}, \widehat{\Theta_2})\right]$ which follows a chi-square distribution with $n_1 - n_2$ degrees of freedom. For more information on MLE, the reader is referred to Hubbert (*16*).

The NGSIM data set allows us to test parameter differences across vehicle types and lanes. The estimation and hypothesis test results are shown in the following sections.

Homogeneity among Vehicle Classes

Table 3 summarizes the estimation results for different vehicle classes. The first three rows in this table give the results for models estimated with data only involving the corresponding vehicle class as the follower, while the last row corresponds to a model estimated with the overall data set, without distinguishing vehicle types. It can be seen that we cannot reject the hypothesis that model parameters are different for different vehicle classes.

Figure 3 shows the 99% confidence intervals (CI) of the estimated values of β, $\tilde{\sigma}$ and α, which can be used to test the equality of these parameter values across vehicle types simply by observing if these intervals overlap or not. It can be seen that the intervals for motorcycles and trucks are much wider than that of passenger cars, which is the consequence of the available sample sizes. It can be seen that the main differences between cars and trucks are in the following parameters:

1. β: Trucks have a higher value than cars for this parameter, which implies that trucks tended to accelerate more aggressively than cars.
2. $\tilde{\sigma}$: Trucks exhibit a higher value, which implies that truck drivers have a larger variation when accelerating, which might be related to the

Table 3. Maximum Likelihood Estimation Parameter Values for Different Vehicle Types

Vehicle class	$\hat{\mu}_\delta$		$\hat{\mu}_\tau$		$\hat{u}$		$\hat{\beta}$		$\hat{m}$		$\hat{\tilde{\sigma}}$		$\hat{\rho}$		$\hat{\sigma}_\delta$		$\hat{\sigma}_\tau$		$\hat{a}$		Log likelihood
	Mean	t-stat	Mean	t-stat	Mean	t-stat	Mean	t-stat	Mean	t-stat	Mean	t-stat	Mean	t-stat	Mean	t-stat	Mean	t-stat	Mean	t-stat	
Motorcycle	5.59	3.6	0.4	3.7	70.09	3.3	90.07	3.6	4.07	3.6	0.24	3.5	−0.49	−5.7	1.68	10.1	1	15.7	0.78	17.9	542
Regular vehicle	7.83	43.2	0.4	27.	76.91	435.2	97.57	3491.6	5.09	104.7	0.13	106.5	−0.03	−0.7	1.07	11.9	0.48	20.1	0.51	186.9	49,716
Heavy vehicle	3.64	0.4	0.42	0.9	73.63	2.4	115.74	19.5	3.27	1.8	0.23	7.5	−0.53	−0.3	1.38	0.2	0.63	1.5	0.95	2.8	455
Overall	7.06	48.4	0.4	22.5	80.9	53.7	107.4	101.1	4.82	31.6	0.08	30.9	0.21	13.3	1.9	15.4	0.31	19.3	0.53	58.3	50,389

Note: Likelihood-ratio test statistic $\Lambda(\mathbf{x}) = 648 > 38 = \chi^2(0.99, 20)$.

number of gears that truck engines use when accelerating.

3. α: Again, this parameter is larger for trucks, and the implications are discussed below.

Of the findings above, the authors believe that the last one is the most significant in relation to the impact of current modeling frameworks. Recall that the parameter α represents the proportion of the gravitational forces because of upgrades that are absorbed by the motion of the vehicle, and has been assumed to be 100% until now. The estimation results show that for regular vehicles $\hat{a} = 0.51$ and for heavy vehicles $\hat{a} = 0.95$. This means that car drivers demand more power from the engine to compensate for gravitational forces such that their actual motion loses only about 50% of what they would have lost had they continued to drive without compensating.

In the case of trucks, we can see that the standard assumption in the literature is appropriate, as they seem to compensate for only 5% of the gravitational force. For motorcycles $\hat{a} = 0.78$ is significantly higher than for regular vehicles, which may seem counter-intuitive since motorcycles have a much higher power-to-weight ratio. A possible explanation is that, precisely for this reason, motorcycles are almost always in the car-following model with little slack for extra acceleration.

Homogeneity among Lanes

Tables 4 and 5 include the estimation results for separate lanes, and Figure 4 shows the CIs of estimated parameter values. It can be seen from Table 4 that the hypothesis that model parameters are different for different lanes cannot be rejected. However, since the estimation results for the three middle lanes are very similar, the hypothesis that the parameters for the three middle lanes are the same was tested and accepted; see Table 5. The slight differences between the vehicles on the three middle lanes are in τ and the way they deal with upgrades, which is implied by the different values of α.

These results accord well with Figure 4, where we can verify that most parameter values are the same for Lanes 2, 3 and 4 since their confidence intervals overlap. It can be seen that the main difference between the middle three lanes compared with the median and shoulder lanes resides in the jam spacing, which is substantially higher in the middle lanes. This can be explained by the higher proportion of trucks and the smaller proportion of motorcycles usually observed in the middle lanes. Another significant difference among lanes can be seen in the middle part of the figure, where the middle lanes exhibit a significantly smaller diffusion coefficient $\tilde{\sigma}$. This implies that in these lanes driver acceleration tends to have less variation than in other lanes. Unfortunately,

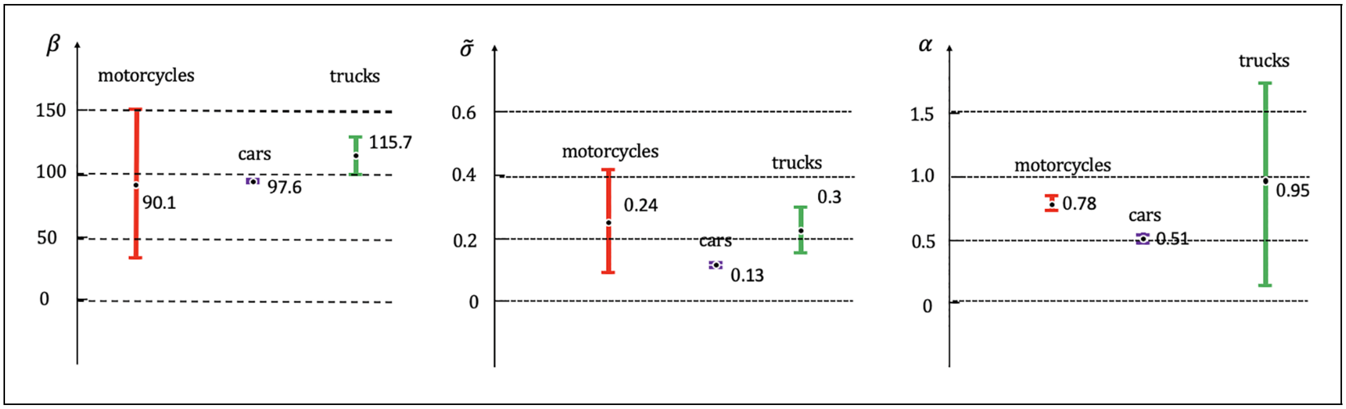

Figure 3. 99% confidence intervals of the estimated values of β, $\tilde{\sigma}$ and α for different vehicle classes.

the explanation that it is because of the higher proportion of trucks does not apply here since we have seen the trucks tend to have a higher $\tilde{\sigma}$. Another possibility is that these lanes exhibit less stop-and-go activity compared with the other lanes and therefore provide fewer opportunities for accelerating in free flow, which is when $\tilde{\sigma}$ can be estimated. The difference of the upgrade parameter α among lanes may be explained by the different vehicle class distribution on each lane. For example, Lane 1 has least percentage of trucks and this may lead to a larger value of the upgrade parameter α compared with other lanes. There is a slight difference between the vehicles on the three middle lanes implied by the different values of α. However, according to the likelihood-ratio test, the parameters are still the same among the three middle lanes. The slight difference in the estimated mean value of α may be caused by the randomness. The confidence intervals of α of the three middle lanes still overlap in Figure 4.

Discussion

In this paper, the authors have used statistical inference based on the maximum likelihood estimation of a two-regime stochastic car-following model using NGSIM data. The main finding pertains to the impact of uphill grades on the acceleration drivers choose to impose on their vehicles. Evidence was found that the current assumption in the existing free-motion acceleration models ($\alpha = 1$) does not apply to car drivers, who tend to overcome half of the gravitational effects by using more engine power. Truck drivers only compensate for 5% of the loss, possibly because of limited engine power; however, more truck data is needed to increase our confidence in these results.

This finding is important for current applications because it means not only that current models are severely overestimating the operational impacts that uphill grades have on regular vehicles, but also underestimating their environmental impacts. For example, the VISSIM model (*17*) uses $\alpha = 1$ and emissions calculations do not consider driver compensation as found here. The emissions and energy consumption for a Honda Pilot 2004 have been calculated with the MOVES model (*18*). In the simulation experiment, the car is accelerating from a complete stop on a 5% uphill segment. The free-flow speed $u = 100$ km/h and the inverse relaxation time $\beta = 0.07$ s $^{-1}$. The results are shown in Table 6. The results show that the current free-motion acceleration models ($\alpha = 1$) are underestimating the environmental impacts by 10% in an acceleration process at uphill grades.

It is also found that the car-following model parameters related to the acceleration process are significantly different among shoulder, median and middle lanes. This can be partially explained by the greater proportion of trucks in the middle lanes, but more data is needed to complete the analysis.

Parameters δ and τ are the key parameters controlling the congested branch in the model. In the model, we assume they follow a BVN distribution, as suggested by Ahn et al. (*12*). From the estimation results, the correlation between δ and τ is found to be zero because the parameter ρ has a low t-statistic. This result is consistent with Ahn et al. (*12*) and indicates that traffic waves propagate as a random walk.

In the authors' previous work (*10*), it was found that if we select $m \approx 1.2$, then the model could replicate both the oscillation and capacity drop. However, the present analysis with the NGSIM data gives a strong indication that the value of m is larger than 3, which means that the acceleration processes of drivers are closer to a Brownian motion than to a geometric Brownian motion. Unfortunately, it also means that the model loses its ability to explain the speed–capacity relationship reported by Yuan et al. (*19*). Research is needed to verify

Table 4. Maximum Likelihood Estimation Parameter Values for Different Lanes

	$\widehat{\mu_\delta}$		$\widehat{\mu_\tau}$		$\hat{u}$		$\hat{\beta}$		$\widehat{m}$		$\widehat{\sigma}$		$\hat{\rho}$		$\widehat{\sigma_\delta}$		$\widehat{\sigma_\tau}$		$\hat{\alpha}$		
Lane ID	Mean	t-stat	Mean	t-stat	Mean	t-stat	Mean	t-stat	Mean	t-stat	Mean	t-stat	Mean	t-stat	Mean	t-stat	Mean	t-stat	Mean	t-stat	Log likelihood
1	4.39	5.5	0.4	3.9	74.0	16.9	92.8	87.6	4.04	14.2	0.16	29.7	–0.29	–6.3	2.	42.	0.67	44.5	0.82	17.1	14,429
2	7.83	36.4	0.4	11.4	76.9	10.2	97.6	5.4	5.08	28.6	0.07	10.4	–0.03	–0.1	1.07	6.6	0.53	16.7	0.47	2.6	12,062
3	7.82	19.5	0.93	41.2	76.9	58.	97.6	19.9	5.08	10.2	0.07	10.5	–0.03	–1.5	1.07	7.9	0.51	57.1	0.45	8.4	10,003
4	7.78	84.6	0.4	30.7	76.9	14.6	97.6	4.6	5.08	6.6	0.07	5.6	–0.05	–0.2	1.08	2.7	0.18	4.6	0.26	2.1	7,844
5	5.35	6.5	0.4	6.7	70.0	28.9	90.0	91.9	2.93	124.5	0.25	18.	–0.55	–0.8	1.79	3.1	0.57	5.1	0.71	17.2	6,430
Overall	7.06	48.4	0.4	22.5	80.9	53.7	107.4	101.1	4.82	31.6	0.08	30.9	0.21	13.3	1.9	15.4	0.31	19.3	0.53	58.3	50,389

Note: Likelihood-ratio test statistic $\Lambda(\mathbf{x}) = 758 > 64 = \chi^2(0.99, 40)$.

Table 5. Maximum Likelihood Estimation Parameter Values for Three Middle Lanes

	$\widehat{\mu_\delta}$		$\widehat{\mu_\tau}$		$\hat{u}$		$\hat{\beta}$		$\hat{\hat{m}}$		$\hat{\hat{\sigma}}$		$\hat{\rho}$		$\widehat{\sigma_\delta}$		$\widehat{\sigma_\tau}$		$\hat{\alpha}$		
Lane ID	Mean	t-stat	Mean	t-stat	Mean	t-stat	Mean	t-stat	Mean	t-stat	Mean	t-stat	Mean	t-stat	Mean	t-stat	Mean	t-stat	Mean	t-stat	Log likelihood
2	7.83	36.4	0.4	11.4	76.9	10.2	97.6	5.4	5.08	28.6	0.07	10.4	–0.03	–0.1	1.07	6.6	0.53	16.7	0.47	2.6	12,062
3	7.82	19.5	0.93	41.2	76.9	58.	97.6	19.9	5.08	10.2	0.07	10.5	–0.03	–1.5	1.07	7.9	0.51	57.1	0.45	8.4	10,003
4	7.78	84.6	0.4	30.7	76.9	14.6	97.6	4.6	5.08	6.6	0.07	5.6	–0.05	–0.2	1.08	2.7	0.18	4.6	0.26	2.1	7,844
Three lanes together	7.81	44.7	0.7	35.1	76.91	207.7	97.57	3102.8	5.08	468.4	0.07	154.4	–0.03	–0.2	1.07	10.	0.51	25.3	0.43	209.5	29,891

Note: Likelihood-ratio test statistic $\Lambda(\mathbf{x}) = 36 < 38 = \chi^2(0.99, 20)$.

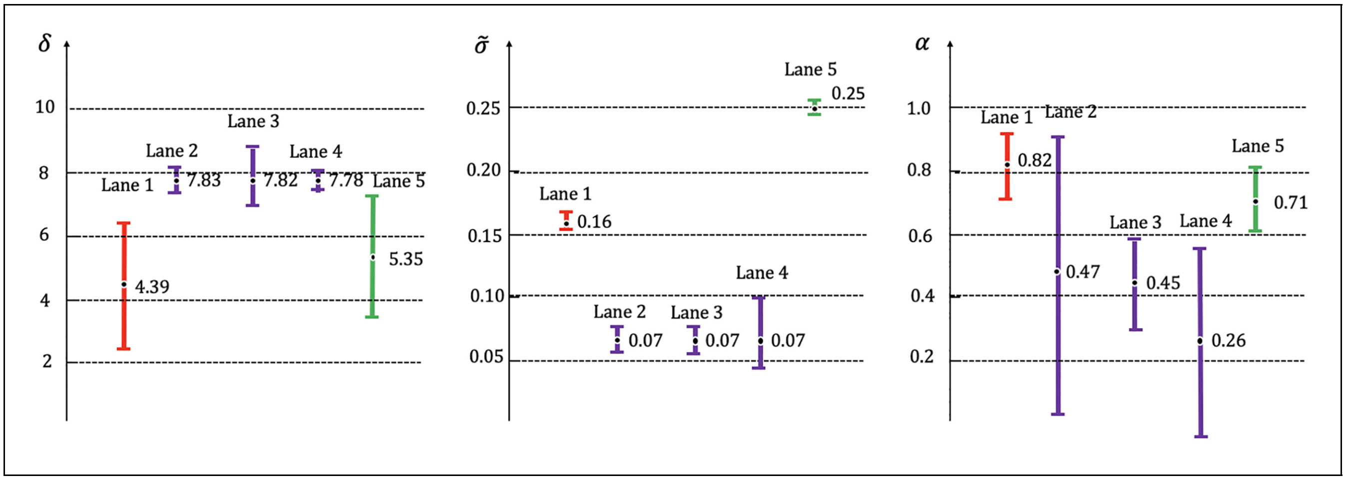

Figure 4. 99% confidence intervals of the estimated values of δ, $\tilde{\sigma}$ and α based on data from five lanes.

Table 6. CO_2 Emission and Energy Consumption Comparison for Different Values of α

	CO_2 emission (gram)			Energy consumption (kJ)		
Distance traveled (meter)	$\alpha = 0$	$\alpha = 0.5$	$\alpha = 1$	$\alpha = 0$	$\alpha = 0.5$	$\alpha = 1$
500	287.7	254	210.1	4,003	3,535	2,924
1,000	484.5	418.9	366.5	6,742	5,816	5,387
2,000	857.4	744.7	673.1	11,931	10,362	9,366

empirically that this relationship exists in the absence of lane changes.

In this paper,

$$a(v) = (u - v(t))\,\beta - gf(G) = (u - v(t))\,\beta - \alpha g \max\{0, G\}, \quad (8)$$

was used to take the roadway upgrade into account, where $gf(G)$ is the acceleration to be subtracted because of grade. However, this formulation assumes a linear relationship between the desired speed and roadway upgrade for the free-flow part of the model, see proposed model 1 in Figure 5. We argue that (i) this relationship may not be linear, (ii) downgrade may also affect the driver's acceleration process, and (iii) roadway grade may also influence the congestion term in the proposed model.

One of the limitations of this study is that a linear model was assumed between vehicle acceleration and roadway grade. However, the impact of roadway grade on the vehicle acceleration may be more complicated. In future research, the authors will estimate different functional forms for $f(G)$ for different values of G, including downgrades. The function $f(G)$ could be piece-wise linear, polynomial or more complex. Some options for $f(G)$ are shown in Figure 5. The authors will carefully compare different models and choose the best fit of $f(G)$ based on various datasets. They also plan to investigate the impact of gradient sequence on vehicle acceleration behavior as an extension of the current work. Also, increasing the sample size of trucks and motorcycles is helpful in the future.

To conclude, this study is based on the statistical inference from a two-regime stochastic car-following

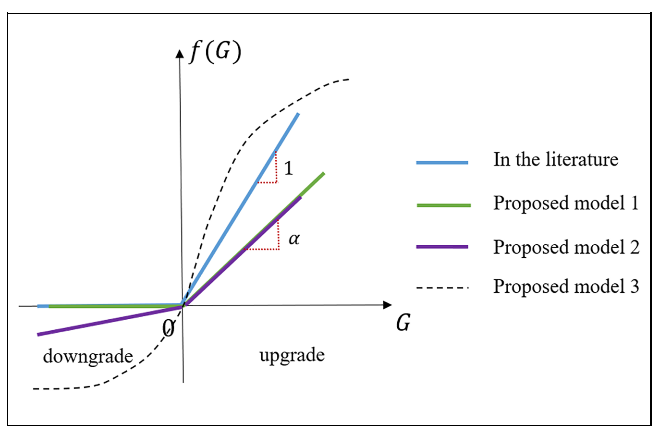

Figure 5. Possible relationships between $f(G)$ and roadway grade in the model.

model and the results are as follows. Car drivers tend to overcome half of the gravitational effects by using more engine power and in doing so, they generate more emissions, while truck drivers are only able to compensate 5% of the acceleration loss because of roadway grade. This study also finds that the acceleration process is significantly different among shoulder, median and middle lanes.

Author Contributions

The authors confirm contribution to the paper as follows: study conception and design: Jorge Laval, Tu Xu; data analysis: Tu Xu; interpretation of results: Tu Xu, Jorge Laval; draft manuscript preparation: Tu Xu, Jorge Laval. Both authors reviewed the results and approved the final version of the manuscript.

Declaration of Conflicting Interests

The author(s) declared no potential conflicts of interest with respect to the research, authorship, and/or publication of this article.

Funding

The author(s) disclosed receipt of the following financial support for the research, authorship, and/or publication of this article: This research was supported by NSF Award # 1826003.

References

1. Walton, M. C., and C. E. Lee. *Speed of Vehicles on Grades*. Technical Report. Center for Highway Research, University of Texas at Austin, TX, 1975.
2. Gillespie, T. D. *Methods for Predicting Truck Speed Loss on Grades*. Technical Report. The University of Michigan Transportation Research Institute, Ann Arbor, MI, 1985.
3. Yu, B. *Modeling Truck Motion Along Grade Sections*. PhD thesis. Virginia Polytechnic Institute and State University, Blacksburg, VA, 2005.
4. The American Association of State Highway and Transportation Officials. *A Policy on Geometric Design of Highways and Streets*. AASHTO Green Book, Washington, D.C., 2011.
5. Laval, J. A. *Hybrid Models of Traffic Flow: Impacts of Bounded Vehicle Accelerations*. PhD thesis. Department of Civil Engineering, University of California, Berkeley, CA, 2004.
6. McLean, J. R. Two-Lane Highway Traffic Operations (TWOPAS). In *Transportation Studies* (Ashford, N., and W. Bell, eds.), Vol. 11. Gordon and Breach Science Publishers, Amsterdam, 1989.
7. Laval, J. A., C. S. Toth, and Y. Zhou. A Parsimonious Model for the Formation of Oscillations in Car-Following Models. *Transportation Research Part B: Methodological*, Vol. 70, 2014, pp. 228–238.
8. Ros, B. G., V. L. Knoop, Y. Shiomi, T. Takahashi, B. van Arem, and S. P. Hoogendoorn. Modeling Traffic at Sags. *International Journal of Intelligent Transportation Systems Research*, Vol. 14, 2016, pp. 64–74.
9. Xu, T., and J. Laval. Parameter Estimation of a Stochastic Microscopic Car-Following Model. Presented at *97th Annual Meeting of Transportation Research Board*, Washington, D.C., 2018.
10. Xu, T., and J. Laval. Analysis of a Two-Regime Stochastic Carfollowing Model: Explaining Capacity Drop and Oscillation Instabilities. *Transportation Research Record: Journal of the Transportation Research Board*, 2019. 2673: 610–619.
11. Newell, G. F. A Simplified Car-Following Theory: A Lower Order Model. *Transportation Research Part B*, Vol. 36, No. 3, 2002, pp. 195–205.
12. Ahn, S., M. Cassidy, and J. A. Laval. Verification of a Simplified Car-Following Theory. *Transportation Research Part B*, Vol. 38, No. 5, 2003, pp. 431–440.
13. James, C., and H. John. *US Highway 101 Dataset Fact Sheet*. Technical Report, FHWA-HRT-07-030. Federal Highway Administration, Washington, D.C., 2007.
14. Liu, H., H. Li, M. Rodgers, and R. Guensler. Development of Road Grade Data using the United States Geological Survey Digital Elevation Model. *Transportation Research Part C: Emerging Technologies*, Vol. 92, 2018, pp. 243–257.
15. Chen, D., S. Ahn, J. Laval, and Z. Zheng. On the Periodicity of Traffic Oscillations and Capacity Drop: The Role of Driver Characteristics. *Transportation Research Part B: Methodological*, Vol. 59, 2014, pp. 117–136. https://doi.org/10.1016/j.trb.2013.11.005.
16. Hubbert, S. *Essential Mathematics for Market Risk Management*. 2nd ed. John Wiley & Sons, Hoboken, NJ, 2012.
17. PTV. User Manual for VISSIM 8. *PTV Group*, 2015.
18. USEPA. *MOVES and Other Mobile Source Emissions Models*, 2019. https://www.epa.gov/moves.
19. Yuan, K., V. L. Knoop, and S. P. Hoogendoorn. Capacity Drop: Relationship between Speed in Congestion and the Queue Discharge Rate. *Transportation Research Record: Journal of the Transportation Research Board* 2015. 2491: 72–80.